Aerospace Systems (2019) 2:97–104
https://doi.org/10.1007/s42401-019-00028-8

ORIGINAL PAPER

Error characteristics analysis and calibration testing for MEMS IMU gyroscope

Pengyu Zhang[1] · Xingqun Zhan[1] · Xin Zhang[1] · Lingxiao Zheng[1]

Received: 15 February 2019 / Revised: 17 April 2019 / Accepted: 27 May 2019 / Published online: 4 June 2019

Abstract
Microelectromechanical systems' (MEMS) inertial measurement unit (IMU) is widely used in many scenarios for its small size, low weight, and low-power consumptions. However, it possesses relatively low positioning accuracy compared with other high-grade IMUs, as errors accumulate quickly over time. This paper mainly focuses on the error characteristics of the gyro part of MEMS IMU by analyzing different kinds of error parameters. As there is no published standard for MEMS gyro error characterization, three dominant error parameters are selected and investigated, namely, scale factor, in-run bias stability, and angular random walk. In addition, Allan variance analysis is deployed as an important part of the scheme with relative results presented in this paper. Not only is theoretical analysis presented, but experimental verification is also carried out correspondingly with an ADIS16490 MEMS IMU. By comparison, we find that the results of in-run bias stability exceed the given features by up to ten times, while the rest of the results agree quite well with the given features. Possible reasons for the exceeding part are given. Calibration testing results not only provide concrete characterization for MEMS gyro errors, but also enhance the importance of overall calibration of MEMS IMU before use.

Keywords MEMS · IMU · Gyroscope · Error characteristics · Calibration · In-run bias stability · Allan variance

1 Introduction

Inertial navigation systems (INS), in many cases, are combined with other navigation aids for better navigation performances. Among various INS sensors, IMU is a sensor assembly constructed with inertial sensors including accelerometers and gyros [1]. The wide usage of IMU covers from aerial navigation to smart phones, thus, resulting in a high demand for IMUs of different types [2, 3]. In this paper, we mainly focus on the gyro part of an IMU. MEMS IMU, a relatively new type, has been used more and more widely because of its small size, low weight, and low-power consumption [4, 5]. However, compared with other types of IMUs, for example, fiber optic gyroscope (FOG), MEMS IMU has lower accuracy, which means that errors accumulate more quickly for a MEMS IMU and navigation solutions are deteriorated in a short time period [6, 7]. This leads to the topic of this research, error characteristics of MEMS IMU, and methods of evaluating these errors [8].

The paper is structured as follows. In the first part, a brief introduction of MEMS IMU is given. Then, the motivation of analyzing the error characteristics specifically for the MEMS IMU is introduced. As for the second part, theoretical analysis of error characteristics of MEMS IMU is performed. Errors of an MEMS IMU are influenced by many factors and can be sorted in many ways [9]. To make the research concise and effective, we choose three main series of error parameters, namely, scale factor, in-run bias stability, and angular random walk. The selection of these three parameters is based on both research hotspots and practical application demands. Other temperature-related and repeatability errors will be in the list of future work. In addition, Allan variance analysis, which was first put forward for oscillator analysis, is also deployed in the calibration scheme [10]. The third part mainly deals with the detailed experiment verification process. It is performed on a turntable with the tested ADIS16490 MEMS IMU. The first section mainly deals with the test setup for lab calibration. For an IMU prepared for calibration experiment, we need to fix it to the turntable. In addition, data collection scheme is important, so a comput-

✉ Xingqun Zhan
xqzhan@sjtu.edu.cn

[1] School of Aeronautics and Astronautics, Shanghai Jiao Tong University, Shanghai, China

ing stick is used for remote control and data collection in the wireless network together with a laptop, which is safe and efficient. Once the testing environment is set up, experiments can be carried out. According to the rotation of turntable, we divide experiments into two parts: position experiments and velocity experiments. The turntable stands still for a certain period of time at a certain attitude under the instructions from the upper computer, which is why we name them position experiments. Correspondingly, in the velocity experiments, the turntable rotates at a series of input angular velocities. In the fourth part, data are processed on MATLAB, and we compare the results with features from datasheet. We find that the experiment results of in-run bias stability exceed the given features by up to ten times, while the other results match quite well with the given features. Detailed analyses of three series of errors are also performed in the meantime. Besides, data smoothing is deployed in in-run bias stability calculation. In the last part, we summarize the work of the whole article and give an outlook of further research.

This work is expected to benefit the community in two ways. First, three dominant series of error parameters concerning positioning accuracy are investigated and analyzed theoretically. Second, calibration experiment process is presented. By comparing results with the given features, we aim to direct the readers to the necessity of calibrating an INS device before actually using it after purchasing them—the values listed in the datasheet may be deteriorated due to different temperature, humidity, and aging effects. This is true even for the most state-of-the-art MEMS IMU. In a word, this research sheds light on both theoretical and practical significance of error characteristics research of MEMS IMU.

2 Error characteristics analysis of MEMS IMU

Apart from differences in basic mechanism between MEMS IMU gyro and a higher grade gyro, say, FOG, the most remarkable feature of MEMS gyro is that it possesses relatively low accuracy. Only when we look deeply into error characteristics of an MEMS IMU can we put forward with methods to mitigate the influences of complicated noises on positioning solutions. For an MEMS gyro, errors may result from environmental factors, for example, temperature. In addition, inherent noises can arise because of inner electric circuit features. Statistically, errors of an IMU can be divided into two types: systematic errors and stochastic errors [11]. Systematic errors refer to those possessing a fixed value, such as zero offsets, scale factors, axis misalignments, etc. Among various systematic errors, in-run bias stability and scale factor are the dominant error sources during INS standalone navigation process. Therefore, these two errors should be taken into account for the simplified MEMS calibration case. Other parameters, such as axis misalignments, may also count, but do not play as important a role as the former two do. As for stochastic errors, such as noises and bias instabilities, these errors can change at every measurement, and they can be modeled and investigated using statistical approach. Quite a few methods have been put forward on the analysis of stochastic errors, such as autocorrelation analysis and power spectral density (PSD), but the most practical and common method is Allan variance [12]. By analyzing the error characteristics of an IMU using Allan variance, we can tell different sources of noises apart.

All in all, to cover both systematic and stochastic errors, three main series of errors are selected for the gyroscope calibration, scale factor series, zero offset series, and angular random walk series. The first series of parameters are calculated through velocity experiments, and the latter two through position experiments. Zero offset series include zero offset and in-run bias stability. Scale factor series include scale factor, fitted zero position, and scale factor nonlinearity. Angular random walk series include five noise parameters using Allan variance analysis. Besides, in-run bias stability and angular random walk are two dominant parameters provided by manufacturers for IMU users on the datasheet, which is another reason why we choose to investigate the errors above.

Measuring zero offset series testing requires long sampling time, such as 1 h, while the angular random walk and scale factor series only require tens of seconds for a single sampling. Although position experiments might sound anterior to velocity experiments, but we need to first calculate scale factor series which is necessary in the calculation of the other two series. Each of the three error parameter series is presented as follows.

2.1 Scale factor series

In this part, we perform velocity experiments and then calculate three parameters for each of three axes of gyroscope, namely, scale factor, fitted zero position, and scale factor nonlinearity.

For each input velocity, calculate the average output angular velocity, denoted as $\overline{F_i}$, $i = 1, 2, \ldots, 22$. Also calculate the average output in the static state before and after rotation, denoted as $\overline{F_s}$ and $\overline{F_e}$.

Therefore, the final average output angular velocity of gyroscope is denoted as $\overline{F_r}$:

$$\overline{F_r} = \frac{1}{2}(\overline{F_s} + \overline{F_e}). \tag{1}$$

$\overline{F_i}$ subtracted by $\overline{F_r}$ is the final average output angular velocity F_i:

$$F_i = \overline{F_i} - \overline{F_r}. \tag{2}$$

For 22 pairs of input and output angular velocities, Ω_i and F_i, $i = 1, 2,\ldots,22$, we can calculate the scale factor K and fitted zero position F_0 using Gaussian fitting on MATLAB. $\hat{F}_i$ is the fitted output angular velocity:

$$\hat{F}_i = K\Omega_i + F_0. \tag{3}$$

Scale factor nonlinearity K_{n} is denoted as follows:

$$K_{\mathrm{n}} = \max\left(\left|\frac{F_i - \hat{F}_i}{|F_{\mathrm{m}}|}\right|\right). \tag{4}$$

F_{m} is the maximum absolute value of output angular velocity.

As can be seen from the definitions above, scale factor is a factor revealing the accordance between input and output angular velocities in dynamic conditions. Ideally, scale factor should be 1 and the fitted zero position should be 0. Scale factor nonlinearity, which reveals dispersion degree of scale factor, should be 0 in ideal conditions.

2.2 Zero offset series

In this part, position experiments are performed. Two parameters are calculated, zero offset B_0 and in-run bias stability B_{s}, with their units °/h instead of °/s, so an extra 3600 should be multiplied in the data processing.

For each axis of gyroscope, zero offset B_0 is calculated using the following formula:

$$B_0 = \frac{1}{K}\cdot\overline{F}. \tag{5}$$

K is the scale factor and $\overline{F}$ is the average output angular velocity of static state.

B_{s} is denoted by the following formula:

$$B_{\mathrm{s}} = \frac{1}{K}\sqrt{\frac{1}{n-1}\sum_{i=1}^{n}\left(F_i - \overline{F}\right)^2}. \tag{6}$$

F_i is the output angular velocity, while n is the sampling number. In addition, we can see in the formula of B_{s} that scale factor K needs to be calculated in advance, so the velocity experiments should be performed ahead of position experiments.

This series of parameters reveals the error characteristics under static state. Zero offset mainly reveals the output with zero input angular velocity, and the value should be 0 ideally. For in-run bias stability, it reflects the degree of deviation of output angular velocity from the zero offset, and ideal value should also be 0.

2.3 Angular random walk series

Using Allan variance model, we can get five parameters related to the device noises. Among them, angular random walk, also called Random Walk Coefficient (RWC), is the most commonly used one.

Allan variance method is introduced in the following contents:

$$\Omega_j(t_0) = \frac{1}{K}F_j(t_0), \quad j = 1, 2, \ldots, n. \tag{7}$$

where t_0 is the sampling interval, which is the reciprocal of sample rate. Then, we put k continuous $\Omega(t_0)$ together as an array. The time span is denoted as τ:

$$\tau = kt_0, \quad k = 1, 2, \ldots, k < \frac{n}{2}. \tag{8}$$

For different k, from 1 to its maximum, calculate the average of each array:

$$\overline{\Omega}_p(\tau) = \frac{1}{k}\sum_{i=p}^{p+k}\Omega_i(t_0), \quad p = 1, 2, \ldots, n-p. \tag{9}$$

Calculate the subtraction of two adjacent array average values, and we denote a new set for a certain τ value:

$$\xi_{p+1,p} = \overline{\Omega}_{p+1}(\tau) - \overline{\Omega}_p(\tau), \tag{10}$$

$$\left\{\xi_{p+1,p},\ p = 1,\ \Lambda\Lambda,\ n-k+1\right\}. \tag{11}$$

For the new set, calculate its standard deviation $\sigma(\tau)$:

$$\sigma(\tau) = \sqrt{\frac{1}{2(n-k-1)}\sum_{p=1}^{n-k-1}\left[\xi_{p+2,p+1} - \xi_{p+1,p}\right]^2}, \tag{12}$$

$$\sigma(\tau) = \sqrt{\frac{1}{2(n-k-1)}\sum_{p=1}^{n-k-1}\left[\overline{\Omega}_{p+2}(\tau) - 2\overline{\Omega}_{p+1}(\tau) + \overline{\Omega}_p(\tau)\right]^2}. \tag{13}$$

For different values of τ, we get a series of $\sigma(\tau)$ correspondingly. In the log–log coordinate system, we can get a curve of $\sigma(\tau)$–τ, which is called Allan variance curve.

It is assumed that the output noises include different components which are independent of each other. Then, $\sigma^2(\tau)$ is the sum of all these noises errors under simplified state. Through least square fitting of the following formula, we get five coefficients from A_{-2} to A_2 corresponding to five noises, respectively.

$$\sigma^2(\tau) = \sum_{m=-2}^{2}A_m\tau^m. \tag{14}$$

Table 1 Corresponding relation between coefficients and noises

Coefficients	Noises	Transformational relation
A_{-2}	Quantizing noise (Q)	$Q = \frac{A_{-2}}{\sqrt{3}}$
A_{-1}	Angular random walk (N)	$N = \frac{A_{-1}}{60}$
A_0	Bias instability (B)	$B = \frac{A_0}{0.6648}$
A_1	Rate random walk (K_r)	$K_r = 60\sqrt{3}A_1$
A_2	Rate ramp (R)	$R = 3600\sqrt{2}A_2$

Table 1 illustrates the corresponding relation between coefficients and noises.

Quantizing noise results from AD sampling. It is a high-frequency noise, which can be easily eliminated and make little difference to navigation accuracy. Angular random walk is influenced by Gaussian white noise, and it is an important index related to navigation performances. Bias instability is another important source of noise which originates from low-frequency oscillation. Rate random walk may be related to aging effects of INS devices, while rate ramp can be eliminated by compensation or strict control of testing environment.

Last but not least, for some beginners in INS, two items, in-run bias stability B_s and bias stability B, may sound alike, especially when they are translated into Chinese. However, they two are totally different with different definitions, calculations and physical meanings. More details will be discussed in part 4 about the proper index reflecting the accuracy of an MEMS IMU.

3 Experimental verification

After analyzing the three main series of error parameters above theoretically, experimental verification is in need, which embodies the error characteristics for a MEMS IMU.

Generally speaking, to evaluate the performances of an IMU of any type, three main practical methods include lab calibration, INS simulation, and field testing [13, 14]. However, when it comes to choosing a suitable method to evaluate the performances of an MEMS IMU, lab calibration is still the most practical and effective way. One reason is that field testing is too expensive and time-consuming for a relatively low-grade MEMS IMU. In addition, lab calibration is an effective way to see whether the features on the datasheet correspond with the performances in real cases. After lab calibration, we may use these calculated parameters in the INS simulation for further research. The MEMS IMU under test is an ADIS16490, and we perform lab calibration with a three-axis turntable for fixation and angular velocity input.

Fig. 1 The charge pal (rectangle silver box), the Intel computing stick (black), and the IMU (the silver one on the upper surface)

This part is divided into two sections. The first section mainly deals with calibration test setup. The second one mainly introduces two series of experiments: position experiments and velocity experiments.

3.1 Test setup for MEMS IMU lab calibration

Putting up an MEMS IMU calibration experiment environment includes the following steps: installing the MEMS IMU onto the turntable, instructing the turntable to rotate, and collecting data from the IMU. Thus, the following contents are allocated in these three parts.

3.1.1 Installing MEMS IMU onto the turntable

The tested device is ADIS16490 MEMS IMU and data are transmitted via USB. As it is not fixed to the turntable originally, we have to fix it to the upper side of the turntable manually. However, it is not practical to connect the IMU with a laptop directly via USB, because rotation of turntable does not allow any wired connection to outside of the turntable. In addition, an external power supply for MEMS IMU itself is required. Therefore, we finally decide to install a charge pal and a computing stick additionally onto the turntable. The charge pal powers the computing stick, while the IMU is connected to the computing stick for both power and data collection. Then, the computing stick is connected to a laptop and controlled using TeamViewer through Wi-Fi. And the final structure of the whole devices is shown in Figs. 1 and 2.

Before installing these parts onto the turntable, some tests are necessary, such as operating time on a single full charge. For the sake of safety, a 5000 mAh charge pal is chosen instead of larger quantity, considering the increasing centrifugal force with increasing electric quantity. Also

Fig. 2 The full view of the experiment environment with IMU, charge pal, and computing stick on the turntable

an external display via HDMI is in need to deal with unexpected problems of the computing stick such as connection failure between computing stick and laptop.

3.1.2 Instructing the turntable to rotate

After we install the tested devices onto the turntable and make sure both IMU and computing stick are ready to work, we can instruct the turntable to maintain a certain attitude or rotate at different angular velocities via the software in the upper computer.

Figure 3 shows the control software of the turntable. This three-axis turntable is of high accuracy, which satisfies the need of MEMS IMU calibration. The attitude simulator can maintain at a certain attitude or rotate at different angular velocities, meeting the needs of the experiment. As can be seen in Fig. 3, when it converts from non-servo state to servo state, the turntable rotates and adjusts automatically, stabilized at a certain state. In addition, it is important to keep a safe distance from the turntable, while it is working.

3.1.3 Collecting data from the IMU

TeamViewer, a remote control software, is installed onto the computing stick before the computing stick is installed onto the turntable. The computing stick is set to connect to Wi-Fi with TeamViewer running automatically, so that it is ready

Fig. 3 The interface of the control software in the upper computer

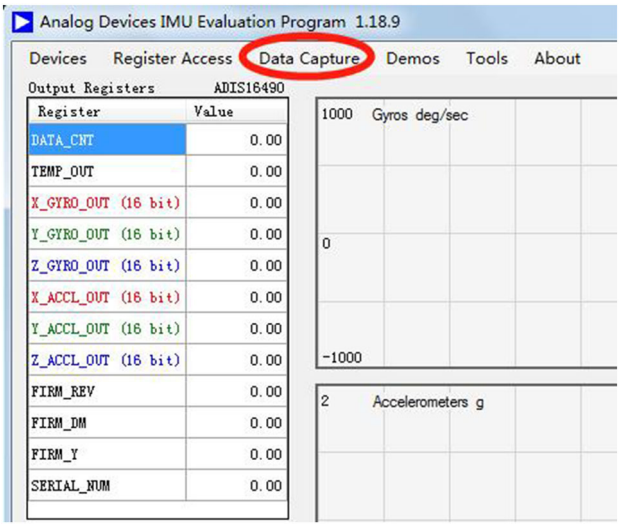

Fig. 4 IMU data client and data capture button

for the connecting to the laptop. Once remote control is connected successfully, we can open the client of MEMS IMU and get ready for data recording.

Figure 4 shows the IMU client and data capture window. Different kinds of parameters can be selected in the final output data, which is saved in the form of CSV document.

3.2 Detailed experiment process

Once we put up the experiment environment, calibration experiments can be carried out according to the specific testing standard. In general, the experiments are divided into two parts: position experiments and velocity experiments.

3.2.1 Position experiments

Just as the name suggests, during the position experiments, we give instructions to the upper computer, so that the turntable stabilizes and maintains a certain attitude. For the calibration of a gyroscope, the testing axis, which is called input reference axis (IRA), should point to the east direction to avoid the effects of earth rotation. For example, in Fig. 2, the x-axis of IMU gyroscope points to the east. And with the changes of turntable attitudes, y- and z-axes can also be turned to east. We set the sampling time for the MEMS gyroscope as 1 h with default sample rate of 4250/s to make the testing results convincing. The data are saved and named, respectively.

3.2.2 Velocity experiments

Velocity experiments refer to the situations where the turntable rotates at a certain angular velocity. In addition, IRA pointing to the east is required. Therefore, we need to first change the direction of IRA to east, and then, we give instructions to the upper computer to make the IMU rotate on the IRA at different input angular velocities.

To reveal the comprehensive performances of MEMS IMU under different input angular velocities, a wide and uniform range of input velocities is selected. According to the datasheet, the maximum input velocity is ± 100°/s, so we set 11 grades of input angular velocity as: ± 5°, ± 10°, ± 20°, …, ± 100°. Sampling time for each single test is set as 30 s, with default sample rate of 4250/s.

In addition, some details have to be noticed. Taking x-axis as an example, at the very beginning of the velocity experiment, we need to record the output velocity of x-axis in the static state for 30 s. Then, instruct the turntable to rotate on x-axis in the following order: 5°/s, − 5°/s, 10°/s, − 10°/s, …, 100°/s, − 100°/s. Then, another 30-s record is needed for the static state.

After testing one axis of gyroscope, IMU needs to be shut off for cooling down and then reconnected to the computing stick. For y- and z-axes, detailed operating steps are similar. The data should be saved and named, respectively.

4 Discussion

Once experiments are performed and results are saved, we calculate three series of parameters according to part 2 using MATLAB. In this part, we compare the results with features from the datasheet to see how well the testing results match with given features. Detailed analysis is presented especially for the results which exceed the given features. Some deductions of the reasons for the exceeding part are given. In addition, small skills when dealing with in-run bias stability are shared with similar researchers. More detailed analysis about Allan variance results is also shown in this part, and finally, we discuss which error index series we should choose when it comes to evaluating the performance of an MEMS IMU.

Table 2 Results of scale factor series

	Scale factor K	Fitted zero offset F_0 (°/s)	Scale factor nonlinearity K_n (%)
x-axis	1.001	− 0.0579	0.33
y-axis	1.0006	0.0658	0.20
z-axis	1.0004	0.0442	0.20

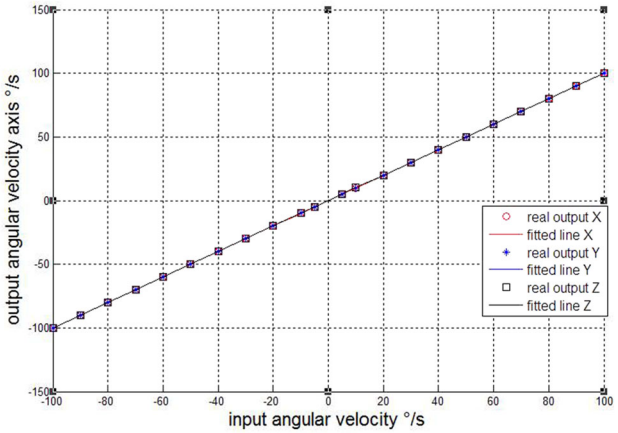

Fig. 5 Real output and fitted output angular velocities of three axes

4.1 Scale factor series

The results are shown in Table 2.

From the results of the experiment, we can see that three K values are very much close to 1. Similarly, F_0 and K_n are very close to zero. All these results show good performances in scale factor series. Figure 5 shows real output and fitted output angular velocities, in which dots represent real ones and line is fitted with F_0 and K_n. As can be seen in Fig. 5, the line matches quite well with the dots for each axis, thus illustrating good performances of scale factor series.

4.2 Zero offset series

The results are compared with given features, and shown in Tables 3 and 4. When processing these two parameters, data smoothing is needed. Here is an example of data smoothing. In this experiment, sampling rate is 4250 Hz, and sampling time is 1 h, that is, 3600 s, which means that we have 15,300,000 data points in all. And sampling interval is 1/4250 s. If we directly use these 15,300,000 points to

Table 3 Results of zero offset series with 1 s smoothing time

	x-axis	*y*-axis	*z*-axis
Zero offset B_0 (°/s)	0.0131	0.0425	0.0808
In-run bias stability B_s (°/h)	17.6690	6.4037	5.9840

Table 4 Results of zero offset series with 100 s smoothing time

	x-axis	*y*-axis	*z*-axis
Zero offset B_0 (°/s)	0.0131	0.0425	0.0808
In-run bias stability B_s (°/h)	17.2156	3.5634	3.3510

Table 5 Results of angular random walk series

	Quantizing noise μ rad	Angular random walk $°/\sqrt{h}$	Bias instability °/h	Velocity random walk $°/\sqrt{h^3}$	Rate ramp $°/h^2$
x-axis	0.16511	0.063866	9.2352	476.05	8223.9
y-axis	0.18133	0.070132	11.25	556.19	9679.7
z-axis	0.17716	0.068629	9.7598	505.63	8621.1

calculate zero offset or in-run bias stability, this is not the so-called data smoothing. We can calculate the average of the output of each certain period of time interval, 1 s, for example. Then, we can get 3600 averages and take them as a new set of samples, and calculate its B_0 and B_s. This process is called data smoothing. In addition, we may choose other smoothing time, like 10 s or 100 s. Here, we compare the results of two smoothing time: 1 s and 100 s. The results are shown in Tables 3 and 4, respectively.

We can see that the values of B_0 do not change as smoothing time varies, while B_s reduces as we prolong smoothing time, which is easy to understand. However, there is no such published standard as for what value the data smoothing time should be set as. Different values of data smoothing time and even the whole testing time may cause the disagreement in calibration results. Therefore, it is recommended that we should set different smoothing time values and compare these results with the given features.

In most cases, the values of in-run bias stability, instead of zero offset, are presented on the datasheet by the manufacturers. Therefore, we pay more attention to in-run bias stability performances, while the zero offset values are only provided as a reference for similar researchers.

As can be seen in Tables 3 and 4, the results of in-run bias stability show larger discretization than the given feature of 1.8°/h, especially in the *x*-axis. One possible reason is that the mechanical oscillation of turntable causes the fluctuations in gyro output. As time goes by, the errors tend to accumulate rapidly. The other reason is that we fix the IMU onto the turntable manually with adhesive tapes and ropes as the condition is limited, which is different from the condition in manufacturers. If we convert to accurate screw fixation in our further research, the value of in-run bias stability could reduce by a certain extent. This also reminds us of the importance of proper installation of IMU devices both in lab calibration and real application scenarios.

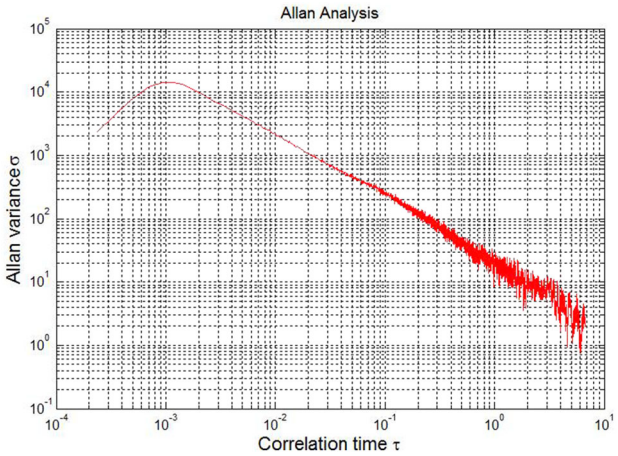

Fig. 6 Allan variance curve of *z*-axis

4.3 Angular random walk series

In this part, the calculated parameters match quite well with the given features of angular random walk, $0.09°/\sqrt{h}$ and are shown in Table 5. Results being smaller than the given features show the good performances of ADIS16490 in eliminating Gaussian white noises. Taking the results of *z*-axis as an example, the Allan variance curve is shown in Fig. 6. The very beginning of the curve can be neglected, because the time is too short. We mainly focus on the curve with its slope approximately − 1/2, and the time period is from 0.001 to 1 s. The slope − 1/2 shows that the main source of noise appears as angular random walk, showing that the gyro is mainly affected by external environmental factors. As time goes beyond 1 s, the curve begins to fluctuate, which means that various sources of noises start to work together.

To sum up, three series of parameters are investigated in this part. The first scale factor series show good dynamic response characteristics of the IMU. As for the second series, a dominant index, in-run bias stability exceeds the given feature, which is likely to result from mechanical oscillation and installation process. Allan variance analysis is presented to calculate angular random walk series, of which angular random walk is one dominant source of noise. In addition, bias instability is often treated as another dominant noise in INS calibration research.

5 Conclusions

In this article, we mainly focus on investigating error characteristics of MEMS IMU specifically. Three dominant error parameters, namely, scale factor, in-run bias stability, and angular random walk, are introduced and analyzed in detail. The selection of these three series is based on the mainstream of both research and application of MEMS IMU. To verify and concretize the error characteristics of MEMS IMU, calibration testing is performed as a supplementary means of research. The whole calibration experiment process is presented in this article from setting up testing environment to analyzing results. The data are processed using MATLAB. In addition, data smoothing is introduced as a small skill when dealing with zero offset parameter series. Finally, a comparison between the experiment results and the given features from datasheet are illustrated in both tables and figures. By comparison, we can see that most results match quite well with the given features for all three series, and notable differences are seen in the in-run bias stability only, with experiment results exceeding the given ones by up to ten times. We deduce that the errors are most likely to originate from installation process. In addition, mechanical oscillation of the turntable is a possible cause for the exceeding error parameters. Allan variance analysis is also deployed as a significant method which leads to angular random walk and bias instability.

As for future work, on one hand, we intend to expand the research to the accelerometer part. On the other hand, more research about error parameters will be under way, for example, those related to temperature and repeatability. We mainly write this paper to analyze error characteristics specifically for MEMS IMU gyro theoretically, and also share the testing results with similar INS researchers.

References

1. Lee D, Lee S, Park S et al (2011) Test and error parameter estimation for MEMS—based low cost IMU calibration. Int J Precis Eng Manuf 12(4):597–603
2. Barbour N, Schmidt G (2001) Inertial sensor technology trends. IEEE Sens J 1(4):332–339
3. Aslan G, Saranli A (2008) Characterization and calibration of MEMS inertial measurement units. In: European signal processing conference. IEEE, Lausanne, Switzerland
4. Hide C, Moore T, Hill C, Abdularhim K (2012) Investigating the use of rotating foot mounted inertial sensor for positioning. In: Proceedings of the 25th ION GNSS, Nashville, 17–21 Sep 2012
5. Zhou Z, Li Y, Zhang J, Rizos C (2016) Integrated navigation system for a low-cost quadrotor aerial vehicle in the presence of rotor influences. J Surv Eng 4:1–13
6. Nassar S, Schwarz KP, El-Sheimy N (2003) INS and INS/GPS accuracy improvement using autoregressive modeling of INS sensor errors. In: Proceedings of the ION NTM, San Diego, 26–28 Jan 2003
7. Shin E, Niu X, El-Sheimy N (2005) Performance comparison of the extended and the unscented Kalman filter for integrated GPS and MEMS-based inertial systems. In: Proceedings of the ION NTM, San Diego, 24–26 Jan 2005
8. Amirsadri A, Kim J, Petersson L et al (2012) Practical considerations in precise calibration of a low-cost MEMS IMU for road-mapping applications. In: American control conference. IEEE, Montreal, QC, Canada
9. Geiger W, Bartholomeyczik J, Breng U et al (2008) MEMS IMU for AHRS applications. In: Position, location and navigation symposium, IEEE/ION. IEEE, Monterey, CA, USA
10. Allan DW (1987) Time and frequency (time-domain) characterization, estimation, and prediction of precision clocks and oscillators. IEEE Trans Ultrason Ferroelectr Freq Control 34(6):647–654
11. Xiaoji N, Qiang W, You L et al (2016) An IMU evaluation method using a signal grafting scheme. Sensors 16(6):854
12. Nassar S (2006) Improving the inertial navigation system (INS) error model for INS and INS/DGPS applications. Ph.D. Thesis, Department of Geomatics Engineering, University of Calgary, Calgary
13. Niu X, Goodall C, Nassar S, El-Sheimy N (2006) An efficient method for evaluating the performance of MEMS IMUs. In: Proceedings of the IEEE/ION position location and navigation symposium, San Diego, 25–27 Apr 2006, pp 1–6
14. Troni G, Kinsey JC, Yoerger DR et al (2012) Field performance evaluation of new methods for in situ calibration of attitude and doppler sensors for underwater vehicle navigation. In: IEEE international conference on robotics and automation. IEEE, Saint Paul, MN, USA